

In-database connected component analysis

Harald Bögeholz
Faculty of Information Technology
Monash University
Melbourne, Australia
harald.boegeholz@monash.edu

Michael Brand
Otzma Analytics Pty Ltd
Melbourne, Australia
research@OtzmaAnalytics.com
Faculty of Information Technology
Monash University
Melbourne, Australia

Radu-Alexandru Todor
UBS
Zürich, Switzerland
radu-alexandru.todor@ubs.com

Abstract—We describe a Big Data-practical, SQL-implementable algorithm for efficiently determining connected components for graph data stored in a Massively Parallel Processing (MPP) relational database. The algorithm described is a linear-space, randomised algorithm, always terminating with the correct answer but subject to a stochastic running time, such that for any $\epsilon > 0$ and any input graph $G = \langle V, E \rangle$ the algorithm terminates after $O(\log |V|)$ SQL queries with probability of at least $1 - \epsilon$, which we show empirically to translate to a quasi-linear runtime in practice.

Index Terms—Big Data, data science, relational databases, SQL, distributed databases, distributed algorithms, graph theory, blockchain

I. INTRODUCTION

Connected component analysis [1], the assignment of a label to each vertex in a graph such that two vertices receive the same label if and only if they belong to the same connected component, is one of the tent-pole algorithms of graph analysis. Its wide use is in applications ranging from image processing (e.g., [2]–[5], to name a few recent examples) to cyber-security (e.g., [6]–[9]). The most well-known theoretical result regarding connectivity analysis is perhaps the Union/Find algorithm [10]–[12], ensuring that labels can be maintained per vertex in an amortised complexity on the order of the inverse Ackermann function per edge, which is the theoretical optimum.

In real-world settings, however, large graphs such as those analysed in Big Data data science are stored on distributed file systems and processed in distributed computing environments. These are ill-suited for the Union/Find algorithm. For example, Union/Find involves following long linked lists, which is inefficient if the items in these lists reside on different machines.

A widely used platform for Big Data processing is Hadoop with its distributed and redundant file system HDFS and the MapReduce framework for implementing distributed computation [13]. Another, more recent distributed computing framework is Apache Spark [14], building on Hadoop HDFS for data storage. These two have in common that algorithms have to be specifically designed for the respective framework.

However, most of the world’s transactional business data is stored natively in large, relational, SQL-accessible databases, and is only treated as graph data in certain contexts. It is therefore beneficial to have an efficient solution for graph

algorithms, and particularly for the connected components algorithm, within the framework of relational databases. Such a solution obviates the need for data duplication in a separate storage system and for supporting multiple data storage architectures. It also avoids the potential for data conflicts and other problems arising from performing data analysis in two disparate systems.

The present paper presents a new algorithm for connected components analysis, Randomised Contraction. It is practical for Big Data data analytics in the following respects:

In-database execution. Our algorithm uses SQL queries as its basic building blocks. It can therefore be natively executed in a relational database, and specifically within the framework of Massively Parallel Processing (MPP) databases [15] where the architecture is designed for efficient parallel processing.

Scalability. Randomised Contraction uses (for any input graph) an expected logarithmic number of queries, running over exponentially decreasing amounts of data. Our empirical results obtained with an MPP database show it to smoothly scale out to Big Data, running, in total, in an amount of time quasi-linear in the input size.

Space efficiency. Typical database maintenance uses some bounded fraction of available space. Therefore, practical in-database algorithms for use on mass data should not create intermediate data that is more than linear in the size of the input. Our algorithm satisfies this criterion.

Our empirical results show that Randomised Contraction outperforms other leading connected components algorithms when implemented in an MPP database. Furthermore, our in-database implementation of one of the algorithms runs faster than the original Spark implementation and uses fewer resources, allowing it to scale up to larger datasets.

The paper is structured as follows: Section II presents related work. In Section III, we describe the problem formally. In Section IV, we discuss naive approaches to a solution and show where they fail. In Section V, we describe our new algorithm, Randomised Contraction, with several refinements, and in Section VI we analyse its theoretical performance. Section VII gives empirical results. A short conclusions section follows. Appendix A presents excerpts of the code used for

experiments. Appendix B gives improved theoretical bounds on graph contraction that may be of independent interest.

II. RELATED WORK

Many researchers have long tried to optimise connected component finding for parallel computing environments (e.g., [16]). Most suited for this pursuit from a theoretical perspective is the theoretical framework of the Parallel Random Access Machine (PRAM) [17], [18]. PRAM algorithms for connected components finding were presented, e.g., in [19]–[21]. In [22], it was noted that randomised algorithms may have an advantage in this problem. The best result obtained by the randomised approach is [23], where a randomised EREW PRAM algorithm is presented that finds connected components of a graph $G = \langle V, E \rangle$ in $O(\log |V|)$ time using an optimal number of $O((|V| + |E|)/\log |V|)$ processors. Its result is always correct and the probability that it does not complete in $O(\log |V|)$ time is at most n^{-c} for any $c > 0$.

However, as observed by Eppstein and Galil [24], the PRAM model is “commonly used by theoretical computer scientists but less often by builders of actual parallel machines”. Its assumptions, which are idealisations of the parallelised computation set-up, do not accurately reflect the realities of parallel computing architectures, making its algorithms unrealistic to implement or not truly attaining the reported performance complexity bounds.

Indeed, the papers that explore connected components algorithms for large-scale practical architectures do so using decidedly different algorithms. The first MapReduce algorithms that run in a logarithmic number of rounds were proposed by Rastogi et al. [25]. Among several variations of new algorithms presented, they report the overall best practical performance for the Hash-to-Min algorithm. This algorithm, however, has a worst case space usage of $O(|V|^2)$. The best known space usage of a MapReduce algorithm is linear in the input size and achieved by the Tho-Phase algorithm by Kiveris et al. [26]. This algorithm, however, takes $\Theta(\log^2 |V|)$ rounds. The Cracker algorithm proposed by Lulli et al. [27] is implemented in Spark and once again improves the number of rounds to $O(|V|)$, but it does so at the expense of increasing the communication cost to $O(\frac{|V| \cdot |E|}{\log |V|})$.

As outlined in the introduction, if the data to be analysed is already stored in a distributed relational database, it is beneficial to be able to run algorithms in-database instead of exporting data to a different platform for analysis. This led to the development of the open source machine learning library Apache MADlib [28]. This library implements, among a small set of other graph algorithms, a connected components algorithm using Breadth First Search. We show in section IV that its worst case behaviour makes it unsuitable for Big Data data science.

Our novel Randomised Contraction algorithm has an efficient implementation in an MPP database and achieves both the best time complexity and space complexity among the above mentioned algorithms. Like the PRAM algorithms of [22], [23], it is randomised. It is guaranteed to terminate and to

do so with a correct answer, and for any given $\epsilon > 0$ guarantees to terminate after $O(\log |V|)$ SQL queries with probability at least $1 - \epsilon$, where $|V|$ is the number of vertices in the input graph. The algorithm’s space requirements can be made linear deterministically, not merely in expectation, and it can be implemented to use temporary storage not exceeding four times the size of the input plus $O(|V|)$. This is at worst a five-fold blow-up, which is within the typical range for standard database operations.

III. PROBLEM DESCRIPTION

A graph $G = \langle V, E \rangle$ is typically stored in a relational database in the form of two tables. One stores the set of vertices V , represented by a column of unique vertex IDs and optionally more columns with additional vertex information. Another table stores the edge set E in two columns containing vertex IDs and optionally more columns with additional edge information. In the context of connected component analysis, graphs are taken to be undirected, so an (x, y) edge is considered identical to a (y, x) edge. For simplicity we present our algorithm such that its only input is an edge table containing two columns with vertex IDs from which the set of vertices is deduced. Isolated vertices can be represented in this table as “loop edges”, (v, v) , if necessary.

The output of the algorithm is a single table with two columns, v and r , containing one row per vertex. In each row v is a vertex ID and r is a label uniquely identifying the connected component the vertex belongs to. A correct output of the algorithm is one where any two vertices share the same r value if and only if they belong to the same connected component. Connected component analysis does not make any specific requirement regarding the values used to represent components other than that they are comparable.

IV. SIMPLE SOLUTION ATTEMPTS

Perhaps the simplest approach to performing in-database connected components analysis is to begin by choosing for each vertex a representative by picking the vertex with the minimum ID among the vertex itself and all its neighbours, then to improve on that representative by taking the minimum ID among the *representatives* of the vertex itself and all its neighbours, and to continue in this fashion until no vertex changes its choice of representative. We refer to this naive approach as the “Breadth First Search” strategy: after n steps each vertex’s representative is the vertex with the minimum ID among all vertices in the connected component that are at most at distance n from the original vertex.

Though the algorithm ultimately terminates and delivers the correct result, its worst-case runtime makes it unsuitable for Big Data. Consider, for example, the sequentially numbered path graph with IDs $1, 2, \dots, n$. For this graph, Breadth First Search will take $n - 1$ steps.

To remedy this, consider an algorithm that calculates G^2 , i.e. the graph over the same vertex set as G whose set of edges includes, in addition to the original edges, also (x, z) for every

x and z for which there exists a y such that both (x, y) and (y, z) are edges in G .

Calculating G^2 can be done easily in SQL by means of a self-join. A tempting possibility is therefore to repeat the self-join and calculate G^4 , G^8 , etc.. Such a procedure would allow us to reach neighbourhoods of radius 2^n in only n steps.

Unfortunately, this second approach does not yield a workable algorithm, either. The reason for this is that in G^k each vertex is directly connected to its entire neighbourhood of radius k in G . For a single-component G , the result is ultimately the complete graph with $|V|^2$ edges. This is a quadratic blow-up in data size, which for Big Data analytics is unfeasible.

Our aim, in presenting a new algorithm, is therefore to enjoy the best of both worlds: we would like to be able to work in a number of operations logarithmic in the size of the graph, but to require only linear-size storage.

V. THE NEW ALGORITHM

We present our new algorithm for calculating connected components, **Randomised Contraction**, by starting with its basic idea and refining it in several steps.

A. The basic idea

Let $G = \langle V, E \rangle$ be a graph. The algorithm contracts the graph to a set of representative vertices, preserving connectivity, and repeats that process until only isolated vertices remain. These then represent the connected components of the original graph.

Denote by $N_G[v]$ the *closed neighbourhood* of a vertex v , i.e. the set of all vertices connected to v by an edge in E plus v itself. Let $G_0 = \langle V_0, E_0 \rangle$ be the original graph.

At step i , map every vertex v to a *representative* $r_i(v) \in N_{G_{i-1}}[v]$. The contracted graph $G_i = \langle V_i, E_i \rangle$ is then constructed as $V_i = \{r_i(v) \mid v \in V_{i-1}\}$ and $E_i = \{(r_i(v), r_i(w)) \mid (v, w) \in E_{i-1} \text{ and } r_i(v) \neq r_i(w)\}$. Note that two vertices are connected in G_{i-1} if and only if their representatives are connected in G_i . In other words, for each connected component of G_{i-1} there is a corresponding connected component in G_i .

Repeat this contraction process until reaching a graph G_k that contains only isolated vertices. At that stage each of these represents one of the connected components of the original graph. Applying all the maps r_i in sequence maps each vertex to an identifier unique to its connected component: the composition of the representative functions $r_k \circ r_{k-1} \circ \dots \circ r_1$ is the output of the algorithm.

Assuming the vertices are ordered, the basic idea for the choice of representatives is to set $r_i(v) = \min N_{G_{i-1}}[v]$. After each contraction step, isolated vertices can be excluded from further computation since each of them is known to form a connected component by itself. If the graph is only represented by its edge set, the removal of loop edges effectively eliminates isolated vertices. This leads to a natural termination condition: the algorithm terminates when the edge set becomes empty. Figure 1 illustrates one contraction step using this idea. The

graph (a) is represented as a list of edges (b). The edge list of the contracted graph (e) is obtained by mapping the representative function over all vertex IDs in this list, eliminating duplicates and eliminating loop edges.

B. Randomisation

The algorithm in the previous section still suffers from the same worst case as the Breadth First Search strategy described in Section IV. Consider a sequentially numbered path graph on n vertices as shown in Fig. 2(a). Each vertex except the first one will choose as its representative the neighbour preceding it. The result of contraction is a sequentially numbered path graph on $n - 1$ vertices. This implies that the algorithm takes $n - 1$ steps until the path is contracted to a single vertex. If, on the other hand, the path is labelled differently, it can contract to $1/3$ of its vertices in the optimal case as shown in Fig. 2(b).

A solution for avoiding worst case contraction is to randomise the order of the vertices. We show in Section VI that the graph will then, in expectation, shrink to at most a constant fraction γ of its vertices, with $\gamma < 1$. We further show that if the randomisation is performed independently at each step, this leads to an expected logarithmic number of steps. As a result, the algorithm behaves well for any input. By contrast, other algorithms that rely on a worst case being “unlikely” are vulnerable in an adversarial scenario where such a worst case can be exploited to an attacker’s advantage.

We remark that vertex label randomisation, critical to our algorithm, would not have aided the simple solution attempts described in Section IV. The complexity of Breadth First Search, for example, is bounded by the diameter of the analysed graph, regardless of how vertices are labelled.

C. Randomisation methods

In a practical implementation, choosing a random permutation of the vertices is itself a nontrivial task, especially in a distributed computing scenario such as an MPP database. One way to achieve this is the **random reals method**. At step i , generate for each vertex v a random real $h_i(v)$ uniformly distributed in $[0, 1]$. The choice of the representative then becomes $r_i(v) = \arg \min_{w \in N_{G_{i-1}}[v]} h_i(w)$.

This method in theory achieves *full randomisation*, a uniform choice among all $|V|!$ possible orderings of the vertices, for which the best performance bounds can be proved (see Appendix B). The advantage of the random reals method over brute-force random permutation generation is that the table of random numbers can be created in parallel in a distributed database. A disadvantage is that this table has to be distributed to all machines in the cluster for picking representatives.

A more efficient idea is to pick a pseudo-random permutation by means of an encryption function on the domain of the vertex IDs. If the vertex IDs are 64-bit integers, a suitable choice is the Blowfish algorithm [29] which can be implemented in a database as a user-defined function. Let e_k denote an encryption function on the domain of the vertex IDs with key k . The **encryption method** then works as follows: at step i , choose a random key k_i . Let

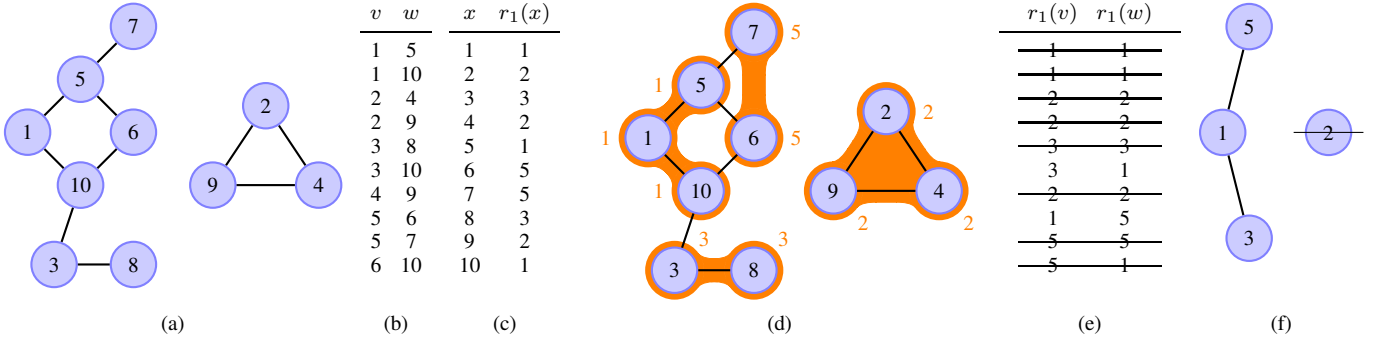


Fig. 1. (a) An undirected graph G_0 with vertex IDs shown inside the nodes. (b) The representation of G_0 as a list of edges. (c) The choice of representative $r_1(x)$ for each vertex x . (d) The graph with representative choices shown at the side of each node. Bubbles around the nodes indicate sets of vertices with the same choice of representative. These will be contracted to single vertices. (e) The edge list of the graph G_1 is computed by mapping the function r_1 over the edge list of G_0 . Duplicates and loop edges, shown struck out, are eliminated. (f) The resulting graph G_1 after one contraction step. The isolated vertex 2, shown struck out, is excluded from further computation.

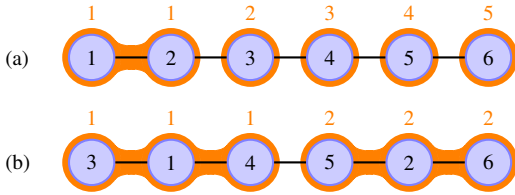


Fig. 2. (a) In a sequentially numbered path graph, every vertex but the first one will choose its left neighbour as a representative. This is the worst case: the contracted graph is only one vertex smaller. (b) If the same path graph is numbered optimally, it contracts to 1/3 the number of vertices.

$r_i(v) = \arg \min_{w \in N_{G_{i-1}}[v]} e_{k_i}(w)$. Note that an encryption function is by definition a bijection which guarantees a unique choice of representatives.

The encryption method is more efficient than the random reals method in a distributed setting since it obviates the need to communicate one random number per vertex across the network to every node that needs it. Instead, only the encryption key needs to be distributed and each processor can compute the pseudo-random vertex IDs independently as necessary. This exploits the fact that in a realistic setting, communication across computation nodes is much slower than local computing.

While encryption functions are designed to be “as random as possible” and work well in practice, it is hard to rigorously prove for them the required graph contraction properties. Also, they are computationally expensive. We therefore present as the final refinement of the Randomised Contraction algorithm the **finite fields method**. Assume the domain of the vertex IDs is a finite field \mathbb{F} with any ordering. To determine the representatives at step i , choose $0 \neq A_i \in \mathbb{F}$ and $B_i \in \mathbb{F}$ uniformly at random and let $r_i(v) = \arg \min_{w \in N_{G_{i-1}}[v]} h_i(w)$ where $h_i(w) = A_i \cdot w + B_i$ with multiplication and addition carried out using finite field arithmetic. Note that h_i is a bijection: in a field, every $A \neq 0$ has a unique multiplicative inverse A^{-1} . If $y = A \cdot x + B$, we have $x = A^{-1} \cdot (y - B)$.

If the vertex IDs are fixed-size integers with b bits, this data type can be treated as a finite field with 2^b elements by performing polynomial arithmetic modulo an irreducible

procedure RANDOMISEDCONTRACTION(G)

```

create table E as
  select v, w from G union all select w, v from G;
firstround  $\leftarrow$  true
repeat
  choose  $0 \neq A \in \mathbb{F}$  and  $B \in \mathbb{F}$  uniformly at random
  create table R as  $\triangleright$  compute representatives
    select v, least(axb(A, v, B), min(axb(A, w, B))) as r
    from E group by v;
  create table T as  $\triangleright$  contract by transforming edge table
    select distinct V.r as v, W.r as w
    from E, R as V, R as W
    where E.v = V.v and E.w = W.v and V.r != W.r;
  rowcount  $\leftarrow$  number of rows generated by the previous query
  drop table E; alter table T rename to E;
  if firstround then
    firstround  $\leftarrow$  false
    alter table R rename to L;
  else
    create table T as  $\triangleright$  compose representative functions
      select L.v as v, coalesce(R.r, axb(A, L.r, B)) as r
      from L left outer join R on (L.r = R.v);
    drop table L, R; alter table T rename to L;
  end if
  until rowcount = 0
  alter table L rename to Result;
end procedure

```

Fig. 3. SQL-like pseudocode for the Randomised Contraction algorithm with deterministic space usage using the finite fields method. axb is assumed to be a user-defined function that computes the term $A \cdot x + B$ using arithmetic over the finite field \mathbb{F} .

polynomial [30, Thm. 3.2.6]. Note that while the calculation of $h_i(w)$ is performed in the finite field \mathbb{F} , the result is stored as an integer and the calculation of $\arg \min$ is done with reference to integer ordering. Since finite field arithmetic over this field is awkward to implement in SQL, we wrote a fast implementation in C and loaded it as a user-defined function into the database. An SQL-only implementation could alternatively choose a prime number p known to be larger than any vertex ID and use normal integer arithmetic modulo p , giving the data type of the vertex IDs the structure of $\mathbb{F} = \text{GF}(p)$.

D. SQL implementation

Our implementation of the Randomised Contraction algorithm in SQL takes as input a table G with two columns, v and w , containing vertex IDs, where each row represents an undirected edge of the input graph. Isolated vertices may be represented in this table as loop edges. The output is a table named *Result* with columns v and r , containing for each vertex v a row assigning a label r to the connected component of v .

Figure 3 shows an SQL-like pseudocode implementation of Randomised Contraction using the finite fields method. It assumes the existence of a user-defined function $\text{axb}(A, x, B)$ that treats a vertex ID x as an element of a finite field and computes the expression $A \cdot x + B$ using finite field arithmetic. Its implementation along with the actual Python/SQL code used for our experiments is given in Appendix A.

At each step, the choice of representatives is computed as a table R . For performance optimisation, we compute the representative as $r_i(v) = \min_{w \in N_{G_{i-1}}[v]} h_i(w)$ instead of using arg min . This runs faster because min is a built-in aggregate function in SQL. Since the values of r_i are no longer vertex IDs of the original graph, the vertices effectively get relabelled at each contraction step. Relabelling does not affect the correctness of the algorithm since the ultimate connected component labels are not required to be vertex IDs, but merely to satisfy uniqueness. Uniqueness is guaranteed by the fact that the functions h_i are bijections on the finite field used as the domain of the vertex IDs.

The contraction step replaces the vertex IDs in each row of the edge table E by their respective representatives, writing the result to a temporary table T . This is implemented by joining the edge table E with one copy of R for each of the two vertices involved. Loop edges are removed from the result to exclude isolated vertices from further computation.

Recall from section V-A that the output of the algorithm is the composition of the representative functions $r_k \circ r_{k-1} \circ \dots \circ r_1$. At step i , the algorithm uses the partial composition $r_{i-1} \circ \dots \circ r_1$ stored in a table L to compute the next partial composition $r_i \circ \dots \circ r_1$ by joining table L with table R . Since isolated vertices get deleted during the course of the algorithm, R represents only a partial function and a left outer join of L and R has to be used to preserve a row for each of the original vertices. Note that the relabelling introduced by the performance optimisation mentioned above has to be applied to all rows of L that do not have a counterpart in R . This is accomplished using the SQL function `coalesce()` which returns its first non-NULL argument.

The algorithm in Figure 3 has deterministic space usage. Table E gets smaller at each step since duplicate edges and loop edges are removed. Table R , containing one row per vertex in E , shrinks accordingly. Table L , however, maintains its size throughout, storing one row per vertex of the input graph.

Figure 4 shows a faster version of Randomised Contraction using slightly more intermediate storage. Instead of joining with the full table L at each step, we first compute and store all

```

procedure RANDOMISEDCONTRACTIONFAST( $G$ )
  create table  $E$  as
    select  $v, w$  from  $G$  union all select  $w, v$  from  $G$ ;
  initialise  $S$  with an empty stack
   $i \leftarrow 0$ 
  repeat
     $i \leftarrow i + 1$ 
    choose  $0 \neq A \in \mathbb{F}$  and  $B \in \mathbb{F}$  uniformly at random
    push  $(A, B)$  onto stack  $S$ 
    create table  $R_i$  as ▷ compute representatives
      select  $v, \text{least}(\text{axb}(A, v, B), \text{min}(\text{axb}(A, w, B)))$  as  $r$ 
      from  $E$  group by  $v$ ;
    create table  $T$  as ▷ contract by transforming edge table
      select distinct  $V.r$  as  $v, W.r$  as  $w$ 
      from  $E, R_i$  as  $V, R_i$  as  $W$ 
      where  $E.v = V.v$  and  $E.w = W.v$  and  $V.r \neq W.r$ ;
     $\text{rowcount} \leftarrow$  number of rows generated by the previous query
    drop table  $E$ ; alter table  $T$  rename to  $E$ ;
  until  $\text{rowcount} = 0$ 
   $(A, B) \leftarrow (1, 0)$ 
  while  $i > 1$  do
     $i \leftarrow i - 1$ 
    pop  $(\alpha, \beta)$  from stack  $S$ 
     $(A, B) \leftarrow (\text{axb}(A, \alpha, 0), \text{axb}(A, \beta, B))$ 
    create table  $T$  as ▷ compose representative functions
      select  $L.v$  as  $v, \text{coalesce}(R.r, \text{axb}(A, L.r, B))$  as  $r$ 
      from  $R_i$  as  $L$  left outer join  $R_{i+1}$  as  $R$  on  $(R_i.r = R_{i+1}.v)$ ;
    drop table  $R_i, R_{i+1}$ ; alter table  $T$  rename to  $R_i$ ;
  end while
  alter table  $R_1$  rename to Result;
end procedure

```

Fig. 4. A faster version of Randomised Contraction with stochastic space usage. axb is assumed to be a user-defined function that computes the term $A \cdot x + B$ using arithmetic over the finite field \mathbb{F} .

representative tables R_i . Each one is smaller than the previous one since it contains only one row for each vertex remaining in the computation. In a second loop, these tables are then joined “back to front” in a left outer join, again taking the necessary relabelling into account.

The result of both algorithms is $r = r_k \circ r_{k-1} \circ \dots \circ r_1$. The algorithm in Figure 3 computes $(r_k \circ (r_{k-1} \circ \dots \circ (r_2 \circ r_1)))$ whereas the algorithm in Figure 4 computes the expression $((r_k \circ r_{k-1}) \circ \dots \circ r_2) \circ r_1$. Note, however, that while the algorithm in Figure 3 guarantees linear space requirements deterministically, the algorithm in Figure 4 only guarantees this in expectation, as shown in Section VI-B. The latter algorithm runs faster because it joins the representative tables in small-to-large order whereas the former one joins with the full-size representative table L at each step.

VI. PERFORMANCE ANALYSIS

A. Time complexity

The critical observation regarding the Randomised Contraction algorithm is that at each iteration the graph shrinks to at most a constant fraction γ of its vertices, in expectation, with $\gamma < 1$. Here we will prove $\gamma \leq 3/4$ for the random reals method and the finite fields method. A better bound of $2/3$ is proved in Appendix B for the case of full randomisation, such as with the random reals method. Note that we only need to consider graphs without isolated vertices since all isolated vertices get removed at the end of each step of the algorithm.

Theorem 1: Let $G = \langle V, E \rangle$ be a graph without isolated vertices. For each vertex v , let $h(v)$ denote either the random real allotted to v by the random reals method or the integer assigned by the finite fields method. Choose representatives $r(v) = \arg \min_{w \in N[v]} h(w)$. Then the expected total number of vertices chosen as representatives is at most $3/4|V|$.

Proof: Divide the vertices into high and low vertices according to the median m of the distribution of a random $h(v)$: the high vertices v are those with $h(v) \geq m$.

For a vertex v to choose a high vertex as its representative, it must (1) itself be a high vertex, and (2) have only high vertices as neighbours. Given that v is not isolated, let us pick an arbitrary neighbour of it, w , and consider a weaker condition than (2): w must be a high vertex. For the random reals method, both conditions occur independently with probability $1/2$. For the finite fields method, let $q = |\mathbb{F}|$. The first condition occurs with probability $\lceil q/2 \rceil / q$ and the second condition, given the first, with probability $(\lceil q/2 \rceil - 1) / q$.

Thus, in expectation, no more than $1/4$ of the vertices choose a high vertex as a representative, proving that in total no more than $1/4|V|$ high vertices will be chosen as representatives. Even if all low vertices are representatives, this still amounts to an expected number of no more than $3/4|V|$ representatives in total. ■

Let γ_i be the actual shrinkage factor at step i of the Randomised Contraction algorithm. This is a random variable with $E(\gamma_i) \leq \gamma$. By re-randomising the vertex order at each step, all γ_i become independent and therefore uncorrelated. This guarantees that the total shrinkage over the first k steps is in expectation

$$E\left(\prod_{i=1}^k \gamma_i\right) = \prod_{i=1}^k E(\gamma_i) \leq \gamma^k.$$

We now show that for any given $\epsilon > 0$ the algorithm terminates with probability $1 - \epsilon$ after $O(\log |V|)$ steps. Let R_k be the random variable describing the number of remaining vertices after k steps. The probability of the algorithm not terminating after k steps is $\Pr(R_k \geq 1)$. By Markov’s inequality we have $\Pr(R_k \geq 1) \leq E(R_k) \leq \gamma^k |V|$. Now $\gamma^k |V| \leq \epsilon \Leftrightarrow k \geq \log_\gamma \epsilon - \log_\gamma |V| = O(\log |V|)$, which is the desired conclusion.

B. Space requirements

The Randomised Contraction algorithm can be implemented in two variants shown in Figures 3 and 4, both using the finite fields method. Both require $\Theta(|E|)$ space for storing the edge table E . Note that the size of this edge table decreases at each step of the algorithm.

The first algorithm uses one table L of size $\Theta(|V|)$ and another table R starting at the same size and strictly shrinking throughout the algorithm, so that space usage for these tables is bounded deterministically by $\Theta(|V|)$. The algorithm shown in Figure 4 stores intermediate tables of expected sizes $|V|$, $\gamma|V|$, $\gamma^2|V|$, \dots , $\gamma^k|V|$, which sums up to a space usage of $\Theta(|V|)$ in expectation.

TABLE I
CONNECTED COMPONENT ALGORITHMS

Algorithm	Number of steps	Space
Randomised Contraction ¹	exp. $O(\log V)$	exp. $O(E)$
Hash-to-Min [25]	$O(\log V)$	$O(V ^2)$
Two-Phase [26]	$O(\log^2 V)$	$O(E)$
Cracker [27]	$O(\log V)$	$O\left(\frac{ V E }{\log V }\right)$

If the random reals method is used instead, both algorithms require an additional $\Theta(|V|)$ for storing a random number for each vertex, which does not change the overall space complexity.

In summary, since $|V| \leq |E|$, the space complexity of the first algorithm is $\Theta(|E|)$ deterministically while it is $\Theta(|E|) + \text{expected } \Theta(|V|)$ for the second algorithm.

In practice, if the algorithms are implemented as shown, the edge table is blown up two-fold in the setup stage. Also, at every iteration, a new edge table has to be generated before the old one is deleted, so, in total, the space requirements for storing edge information during the execution of the algorithm are up to four times the size of its original input.

VII. EMPIRICAL EVALUATION

To evaluate the practical performance of our Randomised Contraction algorithm we used the open source MPP database Apache HAWQ which runs on an Apache Hadoop cluster. Since SQL does not natively support any control structures, we implemented the algorithm shown in Figure 4 as a Python script that connects to the database and does all the “heavy lifting” using SQL queries. Finite field arithmetic over 64-bit integers was implemented in C as a user-defined SQL function.

We compare Randomised Contraction to three other leading algorithms for calculating connected components in a distributed computation setting. Their proven time and space complexities are summarised in Table I. Hash-to-Min and Two-Phase were implemented by their authors in MapReduce [13] whereas Cracker uses Spark [14].

The use of different execution environments and programming paradigms makes a direct comparison of the algorithms difficult. The authors of Hash-to-Min [25] and Two-Phase [26] did not publish original code, and comparison difficulties are further exacerbated by the fact that they did not document their cluster configuration and that [26] provides only relative timing results. We therefore had to port these algorithms to a unified execution environment.

We converted the two MapReduce algorithms and the Spark algorithm to SQL using direct, one-to-one translations. For example, in MapReduce, a “map” using key-value messages was converted to the creation of a temporary database table distributed by the key, and the subsequent “reduce” was implemented as an aggregate function applied on that table. Spark was converted using an equally direct, straightforward

¹Space usage can be made deterministic using the implementation in Fig. 3.

command-to-command mapping. This allows a comparison of different algorithms executing in the same relational database.

For Cracker, we were in addition able to run the original Spark code published in [27] on our cluster. We also implemented our Randomised Contraction algorithm in Spark SQL. This allows a limited comparison between the two execution environments Spark vs. MPP database.

A. Datasets

The datasets used are summarised in Table II. An application to a real-world dataset with nontrivial size is the analysis of the transaction graph of the crypto-currency Bitcoin [31]. At its core, Bitcoin is a data structure called blockchain that records all transactions within the system and is continuously growing.

On April 9, 2019 it consisted of 570,870 blocks with a total size of 250 GB, which we imported into our relational database. Transactions can be viewed as a bipartite graph consisting of transactions and outputs which in turn are used as inputs to other transactions. Each output is associated with an address, and it is a basic step for analysing the cash flows in Bitcoin to de-anonymise these addresses if possible. We used a well-known address clustering heuristic for this [32]: if a transaction uses inputs with multiple addresses then these addresses are assumed to be controlled by the same entity, namely the one that issued the transaction. To perform this analysis, we created the graph “Bitcoin addresses”, linking addresses to the transactions using them as inputs. The connected components of this graph contain addresses assumed to be controlled by the same entities.

We also calculated the connected components of the full Bitcoin transaction graph. This reveals different markets that have not interacted with each other at all within the crypto-currency.

Another important application of our algorithm is the analysis of social networks. We used the “com-Friendster” dataset from the Stanford Large Network Dataset Collection [33], the largest graph from that archive.

Connected component analysis can be used as an image segmentation technique. We converted a Gigapixel image ($69,536 \times 22,230$ px) of the Andromeda galaxy [34] to a graph by generating an edge for every pair of horizontally or vertically adjacent pixels with an 8-bit RGB colour vector distance up to 50. The vertex IDs were chosen at random so that they would not reflect the geometry of the original image.

The same technique can be applied to three-dimensional images such as medical images from MRI scans, or to video. We used a 4K-UHD video of a flight through the CANDELS Ultra Deep Survey field [35] and converted some frames of it to a graph using pixel 6-connectivity (x , y , and time) and a colour difference threshold of 20, again randomising the vertex IDs. By using an increasing number of frames we generated a series of datasets (Candels10 ... Candels160) with similar properties and of increasing size for evaluating scalability of the algorithms.

TABLE II
DATASETS

Dataset	$ V $	$ E $	components
Andromeda	1,459 M	2,287 M	62,166 k
Bitcoin addresses	878 M	830 M	216,917 k
Bitcoin full	1,476 M	2,079 M	37 k
Candels10	83 M	238 M	39 k
Candels20	166 M	483 M	48 k
Candels40	332 M	975 M	91 k
Candels80	663 M	1,958 M	224 k
Candels160	1,326 M	3,923 M	617 k
Friendster	66 M	1,806 M	1
RMAT	39 M	2,079 M	5 k
Path100M	100 M	100 M	1
PathUnion10	154 M	154 M	10

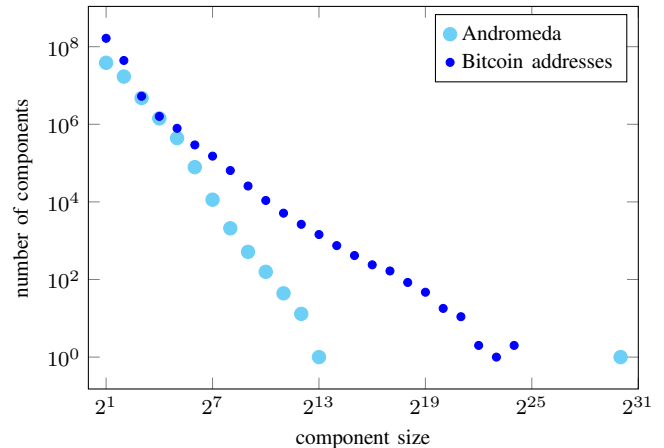


Fig. 5. Connected component sizes exhibit a roughly scale-free distribution for both the Andromeda and the Bitcoin address datasets.

For comparison with [26], we generated a large random graph using the R-MAT method [36] with parameters (0.57, 0.19, 0.19, 0.05), which are the parameters used in [26]. Vertex IDs were randomised to decouple the graph structure from artefacts of the generation technique.

Two worst-case graphs complete our test bench. As shown in the theoretical analysis, Randomised Contraction maintains its logarithmic and quasi-linear performance bounds on any input graph. By contrast, all other algorithms examined have known worst-case inputs that exploit their weaknesses. Path100M is a path graph with 100 million sequentially numbered vertices causing prohibitively large space usage in Hash-to-Min and Cracker. PathUnion10 is the worst case for the Two-Phase algorithm, a union of path graphs of different lengths with vertices numbered in a specific way.

Our 2D and 3D image connectivity datasets are low-degree graphs: each vertex connects only to a handful of other vertices (at most 4 in 2D, at most 6 in 3D). This is a property that holds in a larger class of graphs of real-world interest, such as, for example, street networks.

With the exception of this degree restriction (for the Andromeda and Candels graphs), however, all graphs in our benchmark exhibit traits that are emblematic of the general

TABLE III
RUNTIMES IN SECONDS

Dataset	RC	HM	TP	CR
Andromeda	5431	–	37987	14506
Bitcoin addresses	1530	11696	9811	3457
Bitcoin full	6398	–	77359	26015
Candels10	424	3178	1425	867
Candels20	749	5868	2836	1766
Candels40	1482	13892	6363	3726
Candels80	3463	–	15560	8619
Candels160	9260	–	32615	23409
Friendster	2462	9554	4409	5092
RMAT	2151	4384	2816	3187
Path100M	366	–	1406	–
PathUnion10	386	–	4022	1202

RC = Randomised Contraction, HM = Hash-to-Min
TP = Two-Phase, CR = Cracker

class of real-world large graphs, for which reason we are confident that our results are general.

As an example, consider the distribution of our graphs’ component sizes. Large real-world graphs typically exhibit a property known as scale-freedom. Scale-freedom in component sizes indicates that on a log-log scale a graph exhibits a (roughly) linear relationship between the size of a component and the number of components of this same size. In Figure 5, we demonstrate that the Bitcoin address graph, predictably, shows this log-log linear behaviour.

As can also be seen in Figure 5, however, the corresponding plot for the Andromeda benchmark graph shows the same behaviour, so is, in the relevant metrics, also representative of large real-world graphs, despite its construction from an image. (Notably, the single outlier for Andromeda is the image’s black background.)

B. In-database benchmark results

For performance measurements we used a database cluster consisting of five virtual machines, each with 48 GiB of RAM and 12 CPU cores (Intel Skylake @2.2 GHz), running HAWQ version 2.3.0.0 on the Hortonworks Data Platform 2.6.1. The tests were run on an otherwise idle database.

We have run each of the algorithms three times on each of the target data sets and measured the mean and the standard deviation of the computation time. Like any other parallel processing, in-database execution entails its own inherent variabilities, for which reason we did not expect even the deterministic algorithms to complete in precisely consistent run-times. We did, however, expect the randomised algorithm to have somewhat higher variability in its completion time. Observing the relative standard deviation (i.e. the ratio between the standard deviation and the mean), the average value for Randomised Contraction was 4.0% as compared to 2.2%, 2.1%, and 1.6% for Hash-to-Min, Two-Phase, and Cracker, respectively. We conclude that the variability added by randomisation is not, comparatively, very high.

Table III and Figure 6 show the average runtimes in seconds. Hash-to-Min did not finish on the larger datasets with the

TABLE IV
MAXIMUM SPACE USED IN GB

Dataset	input	RC	HM	TP	CR
Andromeda	59	276	–	115	263
Bitcoin addresses	21	109	88	43	110
Bitcoin full	72	255	–	108	272
Candels10	6	27	21	12	24
Candels20	12	55	42	24	50
Candels40	25	110	86	48	100
Candels80	50	221	–	96	201
Candels160	102	443	–	193	403
Friendster	47	190	183	91	181
RMAT	54	217	120	86	169
Path100M	3	13	–	5	–
PathUnion10	4	20	–	8	20

TABLE V
TOTAL GIGABYTES WRITTEN

Dataset	input	RC	HM	TP	CR
Andromeda	59	552	–	1768	905
Bitcoin addresses	21	215	804	557	306
Bitcoin full	72	690	–	1858	1151
Candels10	6	48	148	93	61
Candels20	12	97	295	179	125
Candels40	25	196	618	369	251
Candels80	50	394	–	774	504
Candels160	102	790	–	1481	1009
Friendster	47	309	481	258	294
RMAT	54	259	248	169	177
Path100M	3	31	–	75	–
PathUnion10	4	48	–	264	116

available resources. Both Hash-to-Min and Cracker cannot handle the Path100M dataset due to their quadratic space usage (on a shorter path of 100,000 vertices they already use more than 100 GB). On all datasets Randomised Contraction performed best, generally leading by a factor of 2 to 12 compared to the other algorithms. On the graph RMAT the advantage was least pronounced.

The sequence of Candels datasets, roughly doubling in size from one to the next, demonstrates the scalability of the Randomised Contraction algorithm. Its runtime is essentially linear in the size of the graph.

Real world space usage of the algorithms has two aspects. One is the maximum amount of storage used by the algorithms at any given time, taking into account the amount of space freed by deleting temporary tables. The other, arguably more important metric for database implementations is the total amount of data written to the database while executing the algorithms.

The latter is significant if the whole algorithm is implemented as a *transaction* in a database. A transaction combines a number of operations into one atomic operation that either succeeds as a whole or gets undone completely (*rollback*). In order to achieve this behaviour, most databases delete temporary tables only at the successful completion of the whole algorithm, and therefore storage is needed for all data written during its execution.

Table IV shows the algorithms’ maximum space usage in comparison with the input size. Here the Two-Phase algorithm uses the least space on all datasets, taking no more than 2 times the storage of the input dataset. Our time-optimised implementation of the Randomised Contraction algorithm stays within the expected bounds and is never more than 2.6 times the space requirements of the Two-Phase algorithm. Table V shows the total amount of data written which would need to be stored in a transaction. Here Randomised Contraction is best in most cases and performs worse only on Friendster and RMAT.

C. Database performance vs. Spark

In [27], Lulli et al. implement Cracker, an optimised version called Salty-Cracker, Hash-to-Min, and several other algorithms in the distributed computing framework Spark [14]. Their published source code is memory intensive and works within our resources only on smaller graphs. Its execution failed on graphs in our test-bench.

For their most highly optimised version of the Cracker algorithm the dataset with the highest runtime was “Streets of Italy” (19 M vertices, 20 M edges). The reported time was 1338 seconds, which was the best among all algorithms compared. We ran our Randomised Contraction algorithm on this same dataset in-database and it finished in 143 seconds. Our database implementation of the Cracker algorithm took 261 seconds.

Note the considerable difference between resources used: the results reported in [27] were obtained on five nodes with 128 GB of RAM and 32 CPU cores each. Our database cluster had less than half the RAM and half the CPU cores. Also the database was configured as it might be in a real-world production environment, never allocating more than 20% of the resources to a single query.

Formulating one’s algorithm in the form of SQL queries also has advantages beyond in-database execution, as it allows utilising it in other SQL and SQL-like execution environments. As an example, we implemented the Randomised Contraction algorithm in Spark SQL using Spark 2.1.1 and ran it on the Candels10 dataset, exported from the database as a distributed set of text files. This allowed the algorithm to scale up properly, but we note that it was still slower in Spark SQL than when executing in the database. The runtime on our cluster was roughly 2.3 times as long for the Spark SQL implementation as for the in-database one, despite both executing the same SQL code on the same hardware. We conjecture that the main reason for this is the higher level of maturity of the query optimisation that databases such as HAWQ provide.

We note that even this factor of 2.3 does not take into account the amount of time required to export the data from the database for analysis or to re-import the results back into the database, operations that would likely be required in a real world implementation.

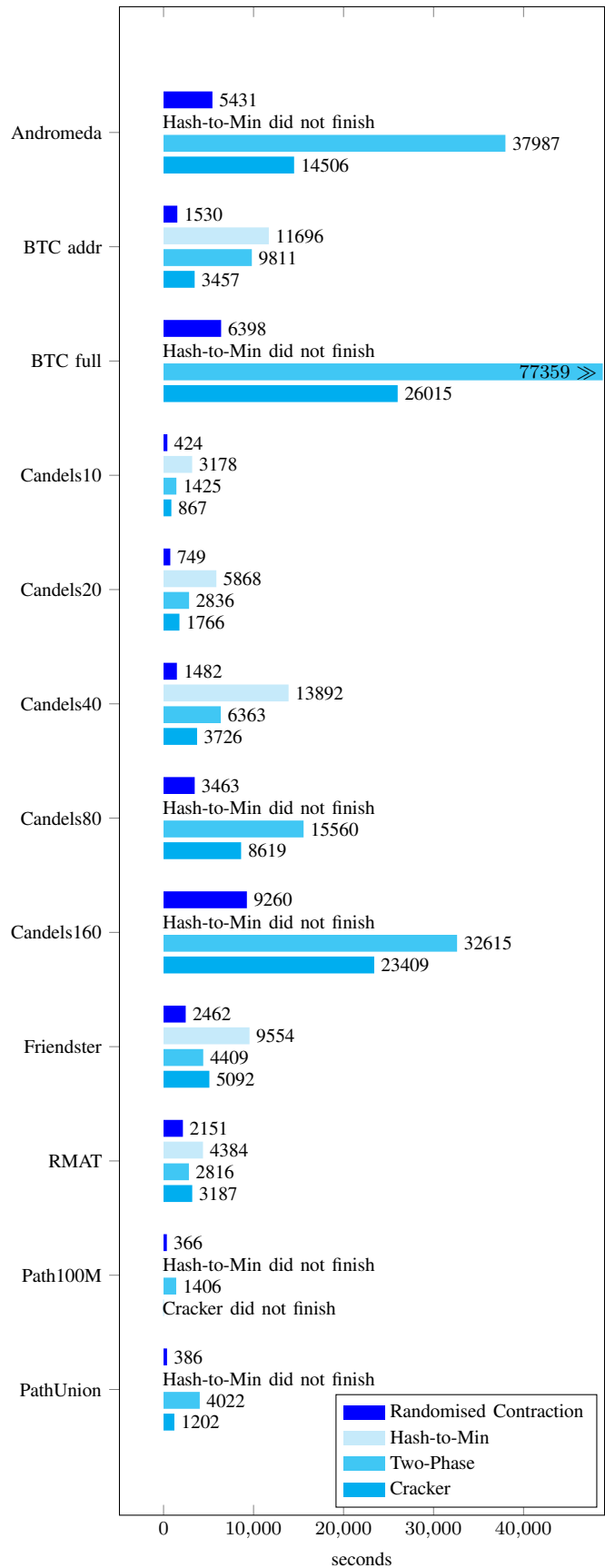


Fig. 6. In-database execution times for real world and synthetic datasets.

```

/* axplusb(a, x, b) calculates a*x+b over GF(2^64).
   Irreducible polynomial: x^64 + x^4 + x^3 + x + 1
*/
#define IRRPOLY 0x1b

PG_FUNCTION_INFO_V1(axplusb);
Datum
axplusb(PG_FUNCTION_ARGS)
{
    int64 a = PG_GETARG_INT64(0);
    int64 x = PG_GETARG_INT64(1);
    int64 b = PG_GETARG_INT64(2);

    int64 r = 0;
    while (x)
    {
        if (x & 1)
            r ^= a;
        x = (x >> 1) & 0x7fffffffffffffff;
        if (a & (1LL << 63))
            a = (a << 1) ^ IRRPOLY;
        else
            a <<= 1;
    }
    PG_RETURN_INT64(r ^ b);
}

```

Fig. 7. The user-defined function axplusb.

VIII. CONCLUSIONS

We describe a novel algorithm for calculating the connected components of a graph that can be implemented in SQL and efficiently executed in a massively parallel relational database. Its robustness against worst case inputs and its scalability make it practical for Big Data analytics. The performance measured is not only due to our algorithm's ability to use a minimum number of SQL queries and to minimise the amount of data handled by each query, but also due to the work of the database's native, generic query execution optimiser.

With relational databases poised to remain the standard for storing transactional business data and with query execution engines improving year to year, the Randomised Contraction algorithm demonstrates that in-database processing can be a viable and competitive addition to the more widely used Big Data processing technologies.

APPENDIX A IMPLEMENTATION IN PYTHON/SQL

In this Appendix we show the implementation of the Randomised Contraction algorithm we used to run the experiments. The user-defined function implementing finite field arithmetic on 64-bit integers in C is shown in Figure 7. It is called from SQL as axplusb(A,x,B) and computes the expression $A \cdot x + B$.

Our Python code is given in Figure 8. It has been stripped of the surrounding infrastructure code. In the excerpt shown, dataset contains the name of the input table which is assumed to contain the edge list of the graph in two columns v1 and v2, each containing a 64-bit vertex ID.

r.log_exec() executes the SQL query passed as the third parameter and returns the number of rows generated. r.log_drop() drops the indicated table. r.execute() executes

```

r.log_exec("setup", 0, """\
create table ccgraph as
select v1, v2 from {0}
union all
select v2, v1 from {0}
distributed by (v1);
""").format(dataset)

roundno = 0
stackA = []
stackB = []
while True:
    roundno += 1
    ccreps = "ccreps{}".format(roundno)
    r_A = 0
    while r_A == 0:
        r_A = random.randint(-2**63,2**63-1)
    r_B = random.randint(-2**63,2**63-1)
    stackA.append(r_A)
    stackB.append(r_B)

    r.log_exec("ccreps", roundno, """\
create table {ccreps} as
select v1 v,
least(axplusb({A},v1,{B}),
min(axplusb({A},v2,{B}))) rep
from ccgraph
group by v1
distributed by (v);
""").format(ccreps=ccreps, A=r_A, B=r_B)

    r.log_exec("ccgraph2", roundno, """\
create table ccgraph2 as
select r1.rep as v1, v2
from ccgraph, {0} as r1
where ccgraph.v1 = r1.v
distributed by (v2);
""").format(ccreps)
    r.log_drop("ccgraph")

    graphsize = r.log_exec("ccgraph3", roundno, """\
create table ccgraph3 as
select distinct v1, r2.rep as v2
from ccgraph2, {0} as r2
where ccgraph2.v2 = r2.v
and v1 != r2.rep
distributed by (v1);
""").format(ccreps)
    r.log_drop("ccgraph2")
    r.execute("alter table ccgraph3 rename to ccgraph")

    if graphsize == 0:
        break

accA = 1
accB = 0

while True:
    roundno -= 1
    (accA, accB) = (r.axplusb(accA, stackA.pop(),0),
r.axplusb(accA, stackB.pop(), accB))
    if roundno == 0:
        break
    ccrepsr = "ccreps{}".format(roundno)
    ccrepsr1 = "ccreps{}".format(roundno+1)
    r.log_exec("result", roundno, """\
create table tmp as
select r1.v as v,
coalesce(r2.rep, axplusb({A},r1.rep,{B})) as rep
from {r1} as r1 left outer join
{r2} as r2
on (r1.rep=r2.v)
distributed by (v);
""").format(A=accA, B=accB, r1=ccrepsr, r2=ccrepsr1)
    r.log_drop(ccrepsr)
    r.log_drop(ccrepsr1)
    r.execute("alter table tmp rename to {}".format(ccrepsr))

r.execute("alter table ccreps1 rename to ccresult")
r.log_drop("ccgraph")

```

Fig. 8. Our implementation of Randomised Contraction in Python/SQL.

miscellaneous SQL queries. $r.\text{axplusb}(A,x,B)$ calls the corresponding function in the database for finite field arithmetic.

APPENDIX B BOUNDS ON GRAPH CONTRACTION

The Randomised Contraction algorithm requires that at each iteration the number of remaining vertices in the graph drops, in expectation, to at most a constant factor γ of the initial number, with $\gamma < 1$. In the body of the paper we prove $\gamma \leq 3/4$, requiring only the weaker form of randomisation that is achieved by the finite fields method. In this appendix we take a closer look at graph contraction under full randomisation and prove a better bound of $\gamma \leq 2/3$ for this case.

To do this, we generalise the problem to directed graphs. We use the following notation [37]: let $G = \langle V, A \rangle$ be a directed graph with n vertices. For a vertex $v \in V$, the set $N^+(v) = \{u \mid vu \in A\}$ is called the *out-neighbourhood* of v and the set $N^-(v) = \{w \mid wv \in A\}$ is called its *in-neighbourhood*. The sets $N^+[v] = N^+(v) \cup \{v\}$ and $N^-[v] = N^-(v) \cup \{v\}$ are called the *closed out-* and *in-neighbourhoods*, respectively.

We represent an ordering of the vertices by assigning to each vertex v a unique label $L(v) \in \{1, \dots, n\}$. The representative of a vertex v under the order induced by the labelling L is defined as $r_L(v) = \arg \min_{w \in N^+[v]} L(w)$.

An undirected graph can be considered as a special case of a directed graph where each undirected edge corresponds to a pair of arcs in both directions. In this case we have $N(v) = N^+(v) = N^-(v)$ for all vertices v and our Randomised Contraction algorithm at each iteration chooses representatives as defined above. The total number of distinct representatives then determines the size of the next iteration's graph and therefore the amount of contraction at each iteration. We note that we do not know of any natural interpretation for the result of running the Randomised Contraction algorithm on a directed graph. Certainly, the output is not a division into connected components.

Given an ordering of the vertices, a vertex can have one of three types: it can be not the representative of any vertex (**type 0**), the representative of exactly one vertex (**type 1**), or the representative of two or more vertices (**type 2+**).

Lemma 1: Let $G = \langle V, A \rangle$ be a directed graph with n vertices. Fix a vertex $v \in V$ with $N^+(v) \neq \emptyset$. Then the number of orderings under which v is of type 1 is less than or equal to the number of orderings under which it is of type 0.

Proof: We prove this by constructing an injective mapping from the labellings that make our fixed vertex v a type 1 vertex to those that make it a type 0 vertex. Consider a labelling L that makes v a type 1 vertex. Then there are two cases: (a) v represents itself and (b) v is the representative of exactly one other vertex.

In case (a) we have $L(v) = \min_{w \in N^+[v]} L(w)$. Let $u_1 = \arg \max_{w \in N^+(v)} L(w)$ and let L' be a new labelling obtained from L by exchanging the labels of v and u_1 . Under this new labelling, v is of type 0: it no longer represents itself and it also does not represent any other vertex because its label is

larger than before. Note that we can uniquely identify u_1 in this new labelling as $u_1 = \arg \min_{w \in N^+(v)} L'(w)$.

In case (b) we have $v = r_L(u_2)$ for some vertex $u_2 \in N^-(v)$ and $r_L(v) \neq v$. Let $u_1 = r_L(v)$. Then $L(u_2) > L(v) > L(u_1)$. Let L' be a new labelling obtained from L by exchanging the labels of v and u_2 . Under this new labelling, u_2 represents itself and v is of type 0: it is no longer a representative of u_2 and it also has not become a representative for any other vertex because its label is larger than before. Furthermore, $L'(u_2) = L(v) > L(u_1) = L'(u_1)$. Note that we can uniquely identify u_2 in this new labelling as the largest-labelled vertex in the in-neighbourhood of v that represents itself. To see this, assume by contradiction that there is a $w \in N^-(v)$ with $L'(w) > L'(u_2)$ and $r_{L'}(w) = w$. Then $u_2 \notin N^+(w)$, $v \in N^+(w)$, and $L(w) = L'(w) > L'(u_2) = L(v)$. From this and the fact that $L(w) = L'(w) = \min_{x \in N^+[w]} L'(x) \leq \min_{x \in N^+[w] \setminus \{v\}} L'(x) = \min_{x \in N^+[w] \setminus \{v\}} L(x)$ we conclude that $r_L(w) = v$. So under the labelling L , v is the representative of two distinct vertices u_2 and w , contradicting the assumption that it is of type 1.

To see that the mapping from L to L' is injective, it remains to be shown that from L' we can uniquely determine whether it was obtained from case (a) or case (b). Let $u_1 = \arg \min_{w \in N^+(v)} L'(w)$ and $u_2 = \arg \max_{w \in N^-(v): w=r_{L'}(w)} L'(w)$. If the latter does not exist, L' must have resulted from case (a). We show that otherwise L' satisfies $L'(u_2) > L'(u_1)$ if and only if it is the result of case (b). We have seen in case (b) that $L'(u_2) > L'(u_1)$. In case (a) we have $L(u_2) = L'(u_2) = \min_{x \in N^+[u_2]} L'(x) \leq \min_{x \in N^+[u_2] \setminus \{v, u_1\}} L'(x) = \min_{x \in N^+[u_2] \setminus \{v, u_1\}} L(x)$ and $L(v) < L(u_1)$. If $L(v) < L(u_2)$, this would imply that $r_L(u_2) = v$, contradicting the assumption that v is of type 1. So $L'(u_1) = L(v) > L(u_2) = L'(u_2)$. We conclude that the two cases cannot produce the same labelling and thus our mapping is injective. ■

We can now prove the central theorem of this Appendix.

Theorem 2: Let $G = \langle V, A \rangle$ be a directed graph with n vertices and for all $v \in V$, $N^+(v) \neq \emptyset$. Let L be a labelling of G chosen uniformly at random. Then the expected number of vertices chosen as representatives by any vertex satisfies $E(|\{r_L(v) \mid v \in V\}|) \leq (2/3)n$. This is a tight bound.

Proof: Let R_0 , R_1 , and R_{2+} be the expected number of vertices of type 0, 1, and 2+, respectively. From Lemma 1 we know that for any fixed vertex v its probability of being of type 1 is less than or equal to its probability of being of type 0, since these probabilities are proportional to the corresponding numbers of orderings. This shows $R_1 \leq R_0$. Using $R_0 + R_1 + R_{2+} = n$, we get

$$2R_1 + R_{2+} \leq n.$$

By counting the number of vertices being represented by each vertex we have

$$R_1 + 2R_{2+} \leq n.$$

Summing the last two equations and dividing by 3 we get

$$R_1 + R_{2+} \leq \frac{2}{3}n,$$

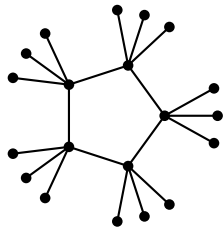


Fig. 9. Graph with highest known contraction factor γ

which is the desired conclusion because $R_1 + R_{2+}$ is the expected number of representatives.

To prove that the bound is tight, consider that $\gamma = 2/3$ is attained when G is the directed 3-cycle. ■

Note that the proven bound is only tight for directed graphs. The worst-case (highest) value of γ for undirected graphs is an open question. The graph with the highest γ value known is the one depicted in Figure 9. It has $\gamma = 81215/144144 \approx 56.343\%$.

ACKNOWLEDGMENT

Portions of the work described in this paper were done while the second author was employed at Pivotal Software, Inc., and are covered by U. S. Patents.

REFERENCES

- [1] J. Hopcroft and R. Tarjan, "Algorithm 447: Efficient algorithms for graph manipulation," *Communications of the ACM*, vol. 16, no. 6, pp. 372–378, 1973.
- [2] K. Kikuchi, Y. Masuda, T. Yamashita, K. Sato, C. Katagiri, T. Hirao, Y. Mizokami, and H. Yaguchi, "A new quantitative evaluation method for age-related changes of individual pigmented spots in facial skin," *Skin Research and Technology*, 2016.
- [3] W. Song, D. Wu, Y. Xi, Y. W. Park, and K. Cho, "Motion-based skin region of interest detection with a real-time connected component labeling algorithm," *Multimedia Tools and Applications*, pp. 1–16, 2016.
- [4] A. Nowosielski, D. Frejlichowski, P. Forczmański, K. Gościwska, and R. Hofman, "Automatic analysis of vehicle trajectory applied to visual surveillance," in *Image Processing and Communications Challenges 7*. Springer, 2016, pp. 89–96.
- [5] X. Wu, P. Yuan, Q. Peng, C.-W. Ngo, and J.-Y. He, "Detection of bird nests in overhead catenary system images for high-speed rail," *Pattern Recognition*, vol. 51, pp. 242–254, 2016.
- [6] A. Giani, E. Bitar, M. Garcia, M. McQueen, P. Khargonekar, K. Poolla *et al.*, "Smart grid data integrity attacks," *Smart Grid, IEEE Transactions on*, vol. 4, no. 3, pp. 1244–1253, 2013.
- [7] G. P. Patil, R. Acharya, and S. Phoha, "Digital governance, hotspot detection, and homeland security," *Encyclopedia of Quantitative Risk Analysis and Assessment*, 2007.
- [8] E. Hogan, P. Hui, S. Choudhury, M. Halappanavar, K. Oler, and C. Joslyn, "Towards a multiscale approach to cybersecurity modeling," in *Technologies for Homeland Security (HST), 2013 IEEE International Conference on*. IEEE, 2013, pp. 80–85.
- [9] M. Yip, N. Shadbolt, and C. Webber, "Structural analysis of online criminal social networks," in *Intelligence and Security Informatics (ISI), 2012 IEEE International Conference on*. IEEE, 2012, pp. 60–65.
- [10] J. E. Hopcroft and J. D. Ullman, "Set merging algorithms," *SIAM Journal on Computing*, vol. 2, no. 4, pp. 294–303, 1973.
- [11] R. Tarjan, "Efficiency of a good but not linear set union algorithm," *Journal of the ACM (JACM)*, vol. 22, no. 2, pp. 215–225, 1975.
- [12] T. H. Cormen, C. E. Leiserson, R. L. Rivest, and C. Stein, *Introduction to Algorithms*. MIT Press Cambridge, MA, 2001, vol. 3, ch. 21.
- [13] D. Miner and A. Shook, *MapReduce design patterns: building effective algorithms and analytics for Hadoop and other systems*. O'Reilly, 2012.

- [14] H. Karau and R. Warren, *High Performance Spark: Best Practices for Scaling and Optimizing Apache Spark*. O'Reilly, 2017.
- [15] D. J. DeWitt and J. Gray, "Parallel database systems: The future of high performance database processing," *Communications of the ACM*, vol. 36, 1992.
- [16] D. S. Hirschberg, A. K. Chandra, and D. V. Sarwate, "Computing connected components on parallel computers," *Communications of the ACM*, vol. 22, no. 8, pp. 461–464, 1979.
- [17] F. E. Fich, "The complexity of computation on the Parallel Random Access Machine," in *Handbook of Theoretical Computer Science, Volume A: Algorithms and Complexity*, J. van Leeuwen, Ed. Amsterdam: Elsevier, 1990, pp. 757–804.
- [18] J. E. Savage, *Models of Computation: Exploring the Power of Computing*, 1st ed. Boston, MA, USA: Addison-Wesley, 1997.
- [19] Y. Shiloach and U. Vishkin, "An $O(\log n)$ parallel connectivity algorithm," *Journal of Algorithms*, vol. 3, no. 1, pp. 57–67, 1982.
- [20] U. Vishkin, "An optimal parallel connectivity algorithm," *Discrete Applied Mathematics*, vol. 9, no. 2, pp. 197–207, 1984.
- [21] B. Awerbuch and Y. Shiloach, "New connectivity and MSF algorithms for shuffle-exchange network and PRAM," *Computers, IEEE Transactions on*, vol. 100, no. 10, pp. 1258–1263, 1987.
- [22] H. Gazit, "An optimal randomized parallel algorithm for finding connected components in a graph," *SIAM Journal on Computing*, vol. 20, no. 6, pp. 1046–1067, 1991.
- [23] S. Halperin and U. Zwick, "An optimal randomized logarithmic time connectivity algorithm for the EREW PRAM," in *Proceedings of the Sixth Annual ACM symposium on Parallel Algorithms and Architectures*. ACM, 1994, pp. 1–10.
- [24] D. Eppstein and Z. Galil, "Parallel algorithmic techniques for combinatorial computation," *Annual Review of Computer Science*, vol. 3, pp. 233–283, 1988.
- [25] V. Rastogi, A. Machanavajhala, L. Chitnis, and A. Das Sarma, "Finding connected components in Map-Reduce in logarithmic rounds," in *Data Engineering (ICDE), 2013 IEEE 29th International Conference on*. IEEE, 2013, pp. 50–61.
- [26] R. Kiveris, S. Lattanzi, V. Mirrokni, V. Rastogi, and S. Vassilvitskii, "Connected components in MapReduce and beyond," in *Proceedings of the ACM Symposium on Cloud Computing*. ACM, 2014, pp. 1–13.
- [27] A. Lulli, E. Carlini, P. Dazzi, C. Lucchese, and L. Ricci, "Fast connected components computation in large graphs by vertex pruning," *IEEE Transactions on Parallel and Distributed Systems*, vol. 28, no. 3, pp. 760–773, 2017.
- [28] J. M. Hellerstein, C. Ré, F. Schoppmann, D. Z. Wang, E. Fratkin, A. Gorajek, K. S. Ng, C. Welton, X. Feng, K. Li *et al.*, "The MADlib analytics library: or MAD skills, the SQL," *Proceedings of the VLDB Endowment*, vol. 5, no. 12, pp. 1700–1711, 2012.
- [29] B. Schneier, "Description of a new variable-length key, 64-bit block cipher (blowfish)," in *International Workshop on Fast Software Encryption*. Springer, 1993, pp. 191–204.
- [30] S. Ling and C. Xing, *Coding theory: a first course*. Cambridge University Press, 2004.
- [31] S. Nakamoto, "Bitcoin: A peer-to-peer electronic cash system," <https://bitcoin.org/bitcoin.pdf>, 2008, accessed: May 27, 2019.
- [32] S. Meiklejohn, M. Pomarole, G. Jordan, K. Levchenko, D. McCoy, G. M. Voelker, and S. Savage, "A fistful of Bitcoins: characterizing payments among men with no names," in *Proceedings of the 2013 conference on Internet measurement conference*. ACM, 2013, pp. 127–140.
- [33] J. Leskovec and A. Krevl, "SNAP Datasets: Stanford large network dataset collection," <http://snap.stanford.edu/data>, Jun. 2014, accessed: Feb 3, 2019.
- [34] NASA, ESA, J. Dalcanton, B. F. Williams, L. C. Johnson, the PHAT team, and R. Gendler, "Sharpest ever view of the Andromeda Galaxy," <http://www.spacetelescope.org/images/heic1502a/>, Jan. 2015, accessed: January 23, 2018.
- [35] NASA, ESA, F. Summers, J. DePasquale, G. Bacon, and Z. L. (STScI), "A flight through the CANDELS Ultra Deep Survey field," <http://hubblesite.org/video/984/science>, Sep. 2017, accessed: January 23, 2018.
- [36] D. Chakrabarti, Y. Zhan, and C. Faloutsos, "R-MAT: A recursive model for graph mining," in *Proceedings of the 2004 SIAM International Conference on Data Mining*. SIAM, 2004, pp. 442–446.
- [37] J. Bang-Jensen and G. Z. Gutin, *Digraphs: Theory, Algorithms and Applications*, 2nd ed. Springer Science + Business Media, 2009.